Statistical Spectral Fitting of the Brown Dwarf Binary System 2M0559

Taran L. Esplin

A senior thesis submitted to the faculty of
Brigham Young University
in partial fulfillment of the requirements for the degree of

Bachelor of Science

Dr. Denise Stephens, Advisor

Department of Physics and Astronomy

Brigham Young University

December 2010

ABSTRACT

Statistical Spectral Fitting of the Brown Dwarf Binary System 2M0559

Taran L. Esplin

Department of Physics and Astronomy

Bachelor of Science

I present the results of a statistical modeling of the near to mid-infrared spectrum of the T4.5 brown dwarf 2MASS J05591914-1404488. The system is over-luminousand and suspected to be a possible unresolved binary but this has not been confirmed observationally. Using a least-squares approach the data is compared to 700,336 single and binary model spectra. I give results for a best single and binary fit. A binary of an unequal mass and temperature (1300K and 1000K) is shown to be a statistically better fit. The best fit predicts cloud formation in the atmosphere of the 1000K secondary. Theoretical justification is given for the presence of clouds in a cool brown dwarf.

Keywords: 2MASS0559, cloud, brown dwarf binary, unequal mass

ACKNOWLEDGMENTS

Dr. Denise Stephens for giving me this opportunity.

Melissa Esplin for her support the semester.

Contents

List of Figures

Chapter 1

Introduction–Binary Brown Dwarfs

Brown dwarfs, objects that typically have spectral classes of M6 and later, are cool, low-mass objects that lack sustained hydrogen fusion in their cores. Though stars can be in class M6 to L4, brown dwarfs are fundamentally different objects. Due to a low effective temperature (T_{eff}), molecules are able to form in the atmospheres becoming a source of wide band spectral absorption. A brown dwarf spectrum is therefore much more complicated than early spectral classes, especially in the near to mid-infrared range, where many simple molecules (CH_4, H_2O, CO, etc.) have strong absorption bands. Grains of complex molecules also form cloud layers at various levels within the atmosphere. The interaction and concentration of molecules depends on many factors and is extremely difficult to model in the laboratory. As such, the theoretical modeling of these systems forms the bases of our understanding of the physical properties of these objects [1]. Unfortunately, most physically observable properties are affected by the convolution of the parameters age, composition, and mass [2]. For example, low-mass, young brown dwarfs can exhibit the same effective temperature as high mass old brown dwarfs. This is due to the failure of brown dwarfs to achieve long-term stability; as a brown dwarf ages it cools and contracts. Mass-luminosity relationships are therefore impossible to define. Thus proposed models need to be tested against observed

spectra for verification (see [3] for an example study).

Brown dwarf binaries give a unique opportunity for study for many reasons. First, accurate orbital parameters produce dynamical mass estimates. Second, the coformation of the system requires equal ages and similar compositions. These two conditions can be used to test evolutionary track models. Known mass, fixed age, and spectra can then establish accurate mass-luminosity-age relations. Most brown dwarf binary systems are equal or near equal mass. However, unequal mass systems, though rare, allow more rigorous testing of evolutionary track models [2].

2MASS J05591914-1404488 (hereafter referred to as 2M0559) is a overluminous T4.5 brown dwarf discovered in 2003 [4]. Parallax measurements give a distance of 10.3 parsecs and tangential velocity of 32.2 km/s [5]. The luminosity can be explained as a binary system but it is presently unresolved and unconfirmed [6]. An equal mass binary spectal fit was previously made but was not shown to be statistically different from a single fit [3].

In this thesis, I will present results of my statistical binary spectral fitting of 2M0559. In chapter 2 I will cover the data reduction process and model prepartaion for the statistical analysis. Chapter 3 will give the results of both single and binary system fits. The system will be shown to best fit a 1300K and 1000K unequal-mass binary. Chapter 4 will discuss the implications of the results and give a theoretical basis of support for the results.

Chapter 2

Observations

2.1 Data type and specifications

Data for this thesis came from the Spitzer Space Telescope archives. Spectral images of 2M0559 taken by previous researchers were downloaded from Spitzer's website through the program "leopard." These images are already processed and it was only necessary to use specific reduced files. These files consisted of bcd, func, and bmask files for each frame. Bcd files are the exposure-level data frames which have been calibrated to absolute flux MJy/sr (a measurement of flux in frequency space). Func images give the uncertainty of each pixel. Bmask files give the probability of each pixel being bad or unusable due to an adverse effect by a known process [7]. These second two files will be used only in IRSClean, a program specifically designed for reducing Spitzer data.

Five individual data runs were done previously of this object. (A data run is a set of frames taken on the same day–Spitzer is a space telescope and a day is defined through universal time.) However, only one set was used in the final data analysis. The other four data runs were taken for a project testing short term differential variability in spectra and therefore no calibration spectra were available. The data used for this study is recorded in

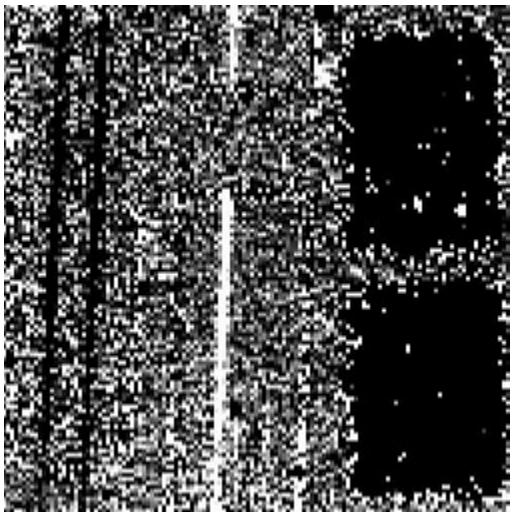

Figure 2.1 An example of a reduced frame showing order and position placement of CCD. In the center is a white line of data in order 2 slit postion 1. Order 1 is in left with the two postions indicated by black lines. Order 3 can be the seen in the center on the top.

the Spitzer archives as program ID 51.

Image frames from Spitzer contained three spectral orders taken at two positions on the slit. Order one contains data from about 7.8 to 14.3μm. Order two contains data from 5.3 to 7.5μm. Order three was not used. The three orders can be seen as the slightly skewed rectangles lightly outlined in white in Fig. 2.1. Order one is the left most box with the two black lines that resulted from a sky subtraction of this image. (Postion one is the left most.) Order two is the lower central box with the white line of spectral data located in position one. Order three is the upper central box with a small white line of data. The other two boxes of black pixels are for direct imaging of objects and were not used for this study. Extracted spectra for the range of 0.8 to 2.5μm was obtained from previous work on this object from Dr. Denise Stephens.

2.2 Reduction

Although the images were already processed, further reduction was needed for the highest quality extracted spectrum. The reduction process used by Dr. Stephens on previous Spitzer spectra was originally given as a step by step procedure. However, an upgraded version of SMART (the extraction program used, see below) necessitated several corrections to the procedure. These changes were identified by myself and approved by my mentor.

1. The first step in data reduction was to find and flag bad pixels in each frame. This procedure eliminated the outlying fluctuation of individual pixels. Numerous processes can be responsible for a bad pixel in a frame. For example, pixels can grow hot over the data run giving false values for the last few frames of a data run.

   (a) Each bcd frame's pixel values were extracted to frame-specific comma separated value files (csv).

   (b) I wrote a program for Matlab to stack the csv file of each image and analyze the files for bad pixels. Results were used to create mask files for the individual frames called "specfix" files (see appendix A.1).

      i. Each pixel has a two dimensional identifier (the X and Y location corrdinates in the frame). Two pixels are considered similar if they have the same identifier but are from different frames with the same order and slit position.

      ii. Then pixels that have a value of zero are eliminated as they skew the statistics.

      iii. The median and standard deviation for similar pixels are taken. Then a median (medianall) and standard deviation (stdall) is taken of all the medians. Each similar pixel median and standard deviation is then labeled "good" if the median value lies within five stdall values from medianall. Otherwise that pixel identifier is labeled "bad."

iv. A new standard deviation is taken of the "good" standard deviations and is called "sigma."

v. Each individual pixel from each frame, irregardless of whether the similar median value is "good," is then labeled "good" if the pixel's value lies within five sigma values from the median of all similar pixels (not meadianall). All others are labeled "bad."

vi. "Specfix" text files are then created for each frame which list the bad pixels identifiers and the similar median value.

vii. The program also creates "mask" text files but due to changes in the later procedure, these files are not used at a later step.

2. For the next step bad pixel values were replaced and zero valued pixels were eliminated from the bcd frames.

   (a) Using a Fortran program previously created by Dr. Stephens, the specfix files were converted into text files. In this form IRAF can then convert the files into fits images.

   (b) IRAF image combining functions were then used to replace the bad pixel values with the correct median values recorded in the the specfix files.

   (c) The zero valued pixels are then eliminated through a linear interpolation routine in IRAF.

      i. A horizontal fit is done for pixels in the sky (non-data holding pixels). A horizontal line of pixels are all approximately the same wavelength. As background radiation can be wavelength dependent, a horizontal linear fit is best

      ii. A vertical fit is done for pixels directly on the spectral data. Spectral data on the frame is physically only 2 to 3 pixels wide (see Fig. 2.1) and therefore

a horizontal approximation over a pixel would include some sky values and artificially create a lower flux value.

3. The frames were now ready for final cleaning and extraction. The rest of the procedure is completed through the program SMART (an IDL based program). This program is specifically designed for Sptizer data. SMART automatically accounts for the slight skewing of the spectral data on the CCD (see Fig. 2.1). The normal IRAF routine is also capable of a skewed extraction but would have been much more difficult to accomplish.

   (a) The func, bmask, and bcd files for each frame were uploaded into SMART.

   (b) Every file is then given a final cleaning through the internal program IRSClean.

   (c) The clean files are then combined into a 3-plane image so the extraction routine can utilize all information from the func, bmask, and bcd files. (The combining routine automatically combines the associated bmask and func images with the appropriate bcd.)

   (d) Sky images are then created by combining images. Sky images are used for eliminating the background radiation that is present (even space telescopes need these).

      i. All the frames with the same order (both positions) are combined by making a new frame where each pixel is the median value of the considered frames. The 2^{nd} order combined image becomes the 1^{st} order sky image and visa versa.

      ii. The sky images are then subtracted from each frame for the associated orders.

      iii. Fig. 2.1 shows the evidence of this subtraction. The 1^{st} order box has dark lines from the subtraction but the 2^{nd} order has an easily identified vertical spectral line.

(e) Data was extracted with a manually identified fixed rectangular column. This column traces the skewed line of data vertically along the CCD frame.

i. The width of the rectangle was 3.0502 measured in pixels centered on the peak. This size is used to obtain the maximum amount of data extracted while avoiding the noise along the edge of the data.

ii. Each position in each order needs to have a peak position identified. I chose the center positions graphically inside the GUI. The GUI automatically labels this pixels internally (see Fig. 2.2). I report the GUI pixel label for central peak position.

A. Order 1 position 1 was centered on pixel -4.637

B. Order 1 position 2 was centered on 5.600

C. Order 2 position 1 was centered on -4.450

D. Order 2 position 2 was centered on 5.384

iii. An example window of the the GUI used to extract is given in Fig. 2.2 showing a 2^{nd} order position 2 extraction in process.

A. The red rectangle shows the defined extraction window.

B. The green dotted lines are manually defined "sky" parameters used by the extraction program.

iv. Due to a program bug 3^{rd} order spectra has to be extracted at the same time as the 2^{nd} order. These data points are not very reliable and are later deleted from the combined spectra.

v. These manually defined parameters are then applied to all similar frames completing the extraction process (see Fig. 2.3 for an example extracted spectra).

4. Before the spectra could be combined, one final calibration was needed. Each individual

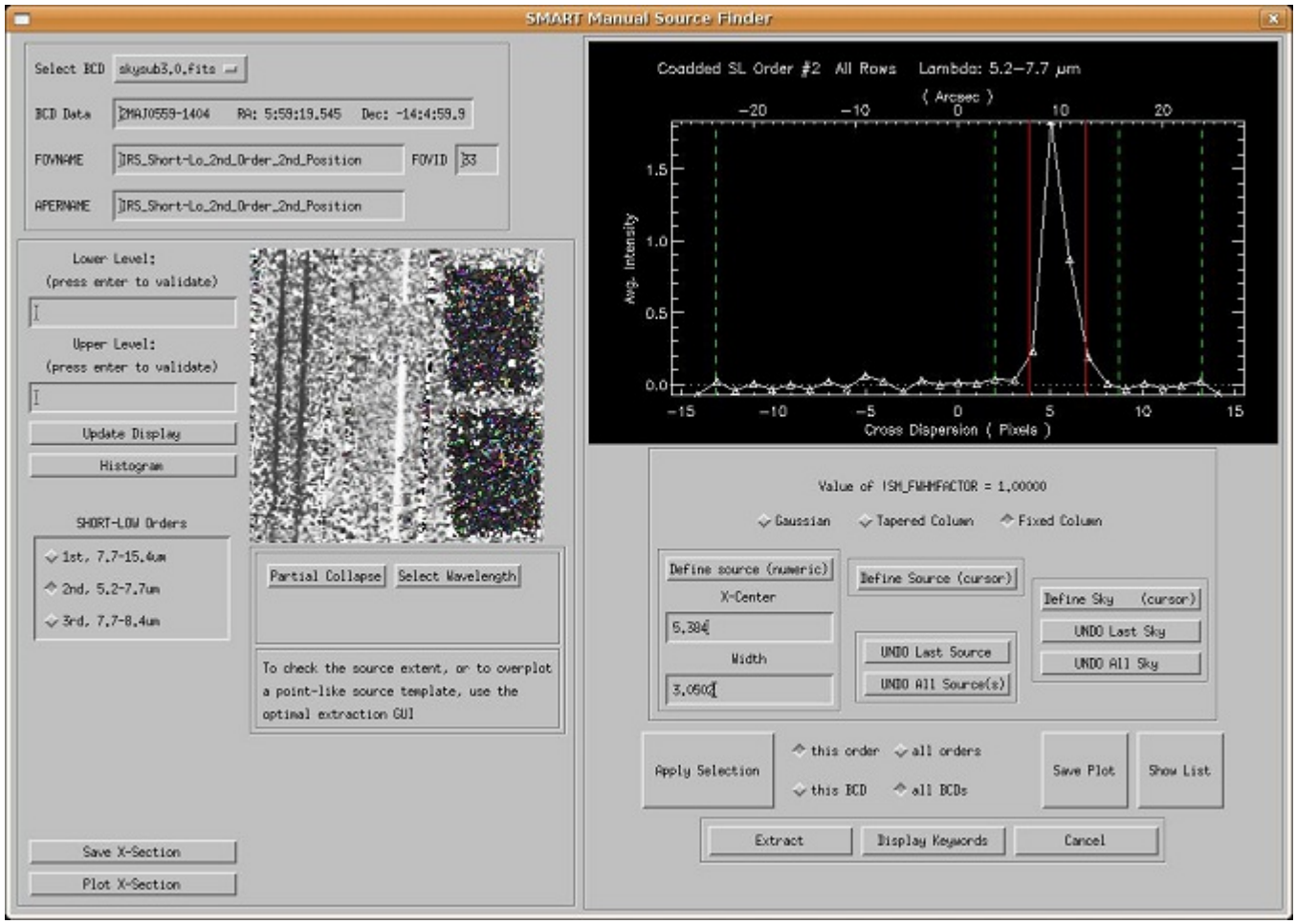

Figure 2.2 A screen shot of the extraction GUI inside of SMART. Pictured is a 2^{nd} Order position 2 extraction is in process.

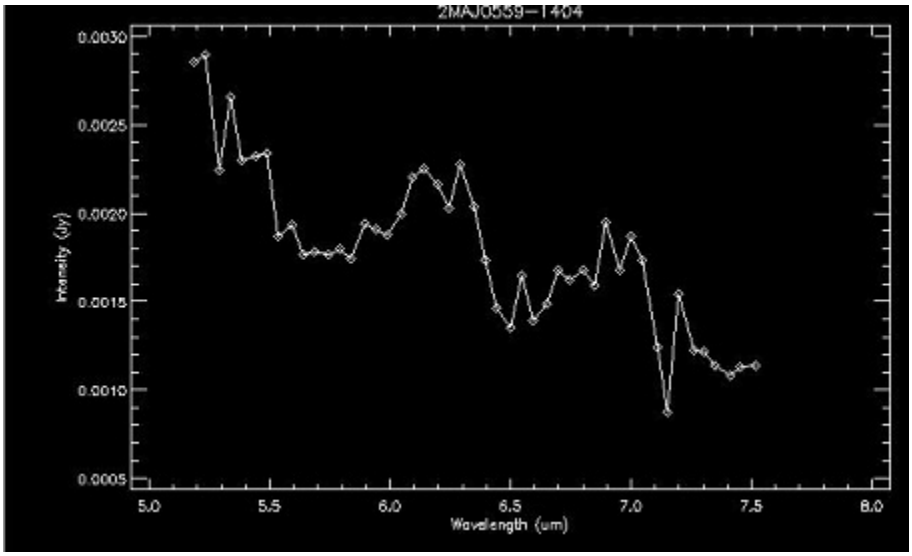

Figure 2.3 A typical spectrum extracted by SMART

pixel on the CCD has an individual response to received flux that can change over the course of a day or two. To correct this problem, every few days Spitzer took spectra on the hot, featureless star HR6348. These frames can be turned into Relative Spectral Response Functions (RSRF) that are used as calibration standards.

(a) Func, bmask, and bcd files were downloaded by leopard for HR6348 from the closest days before and after the original data was taken.

(b) Steps A through C from this procedure were completed for all four order and position permutations.

(c) Inside SMART's spectra manipulation GUI IDEA, high resolution model spectral of HR6348 is rebinned to a reference scale of the appropriate lower resolution. (The reference scale is the Spitzer spectral data taken of HR6348 position and order specific.) The rebinned model is then divided into the corresponding extracted HR6348–once again position and order specific. These are the RSRFs.

(d) Each individual spectra is then multiplied by the appropriate order and position

RSRF. The data is now calibrated.

5. The final step is to combine the data to get one average spectra for 2M0559 inside IDEA.

   (a) Each individual spectra was first trimmed for quality (inside IDEA the processes is called zap). This is done because the sensitivity falls off at the edges of each order.

      i. 1st order had the first two data points zapped (near the 8μm end) and all points after 14.5μm.

      ii. 2nd order had first 4 points (near 5μm end) and the last 2 zapped.

   (b) The two positions in a specific order were then combined by evaluating a mean for each point.

   (c) A set of previously reduced near-infrared from 1 to 2.5μm data was then uploaded into SMART and pieced together with the other data creating a finished spectrum

   (d) This spectrum was then exported into a csv file for analysis.

2.3 Models

2.3.1 Parameters

1184 raw atmosphere models were obtained from Saumon and Marley 2008 [8]. These models were constructed with four variable parameters: effective temperature (T_{eff}); gravity (log g); cloud parameter (f_{sed}); and vertical mixing (K_{zz}). Temperatures for the models spans from 500K to 2400K in increments of usually 100K. Gravity, measured as log g in cgs units, ranges from 4 to 5.5. The cloud parameter is essentially an indicator of particle density in

clouds. $F_{sed} = 1$ implies a high density, $f_{sed} = 4$ is low and no clouds (nc) is where density is approximately zero. This parameter is a artificial indicator of the small scale updrafts in the atmosphere balancing with gravity, keeping the grains aloft that form clouds. Density is maintained at an equilibrium as grains are formed and some grains fall out as "rain." For more information on f_{sed} see Ackerman and Marley 2001 [9]. K_{zz} is a measurement of the speed of large scale vertical mixing within the atmosphere. In a high vertical mixing system NH_3 and CH_4 molecules, which form slowly in the upper atmosphere, are pulled lower in the atmosphere where the higher temperature quickly converts the molecules into N_2 and CO. This effect causes a reduction in the strength of the expected NH_3 and CH_4 absorption bands. The four values in these models are 0, $10^2, 10^4, 10^6 cm^2/s$ (labeled K0, K2, K4, K6) and correspond to different rates of mixing. The numerous models were created by simple permutations of the parameters.

2.3.2 Manipulation

Due to the high resolution of the models compared to the actual data spectra, the models needed to be smoothed to the same resolution. Resolution is the relation between the change of wavelength to wavelength defined through the equation $R = \lambda/\Delta\lambda$. On the CCD, the pixels that record the spectral information are not infinitely thin. The width of wavelengths covered by each pixel relates to the resolution. By smoothing the models to a lower resolution, this becomes a better match of the resolution of Spitzer's spectrograph. I wrote a smoothing program in Matlab (see appendix A.2) to take what is called a variable boxcar average. The width of the boxcar, the $\Delta\lambda$ defined above, is set as a function of wavelength. Each data point in the model spectra is replaced with a mean flux value calculated from the surrounding points with a window R=120, centered on the point to be replaced. The program was ran twice on all the models. This resolution was discovered to be too low for fitting to Spitzer

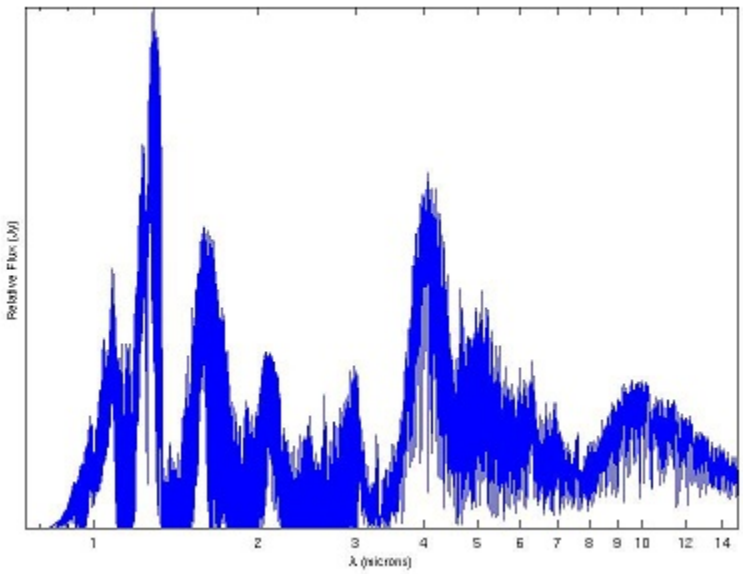

Figure 2.4 An example of high resolution spectra.

data. However, only a few fine absorption features are lost and large scale fitting is not effected. This resolution was used for identifying the top 49 binary fits.

The spectrum used in this study is made from data with two very different resolutions (for 1 to 2.5μm data R=2000-10000, for 5 to 15μm data R=60-120). This necessitates the need for a piecewise model resolution as well. A more correct resolution (appendix A.3) has a window length of R=400 for less than 3 microns and R=60 for greater than 3μm. The choice of 3μm was made because there is a large hole in the data from 2 to 5μm. Fig. 2.4 and Fig. 2.5 gives a comparison between a high resolution model and the same model smoothed to the appropriate resolution. This smoothing procedure was used for the 33 models flagged for fine spectral fitting.

Another Matlab program was written to rebin the models so that there would be a one-to-one correlation to the data spectra (see appendix A.4). The program collapses the smoothed model's many data points down to a mean flux value for every corresponding actual data

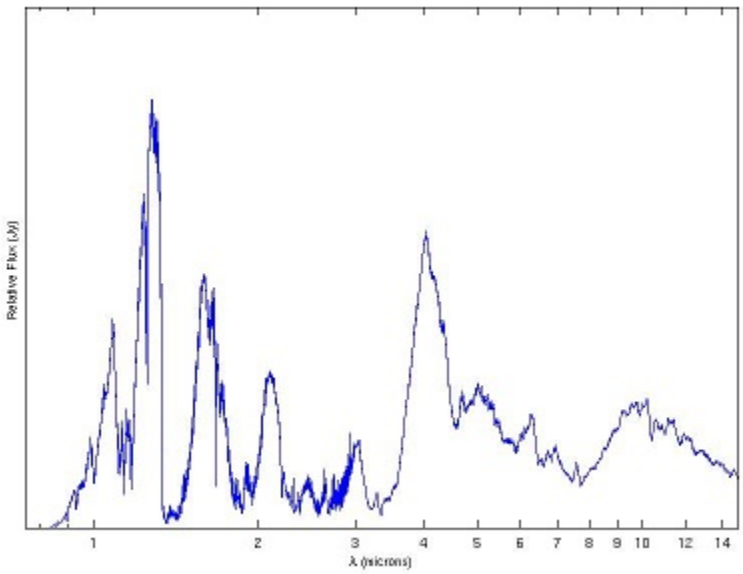

Figure 2.5 An example of smoothed spectra with R=400 from 1 to 3μm and R=60 from 3 to 14μm.

point. In this form the models were ready for analysis.

Chapter 3

Analysis

3.1 Statistical Approach

I used a least squares approach to find a best single and binary fit to 2M0559. The basic fitting function is defined in equation 3.1.

$$G1 = \sum_i w_i (F_i - \mathbf{x} \ . \ \mathbf{f_i})^2 \tag{3.1}$$

The summation is done over every data point. The statistical weighting factor (w_i) was set to be the wavelength divided by the mean flux value for the entire model. This factor is necessary due to the extreme differences in order of magnitude in the models. Without the mean model flux the lowest temperature model has the best G value despite its obviously incorrect fit. The wavelength was also used in the weighting factor to correct for the high density of near-infrared data points compared to the mid-infrared density. $\mathbf{F}_i$ and $\mathbf{f}_i$ was the flux densities of model and data respectively. Theoretically, the vector $\mathbf{x}$ represents the distance and radial dependence of measured flux densities. In this analysis $\mathbf{x}$ was varied to minimize G.

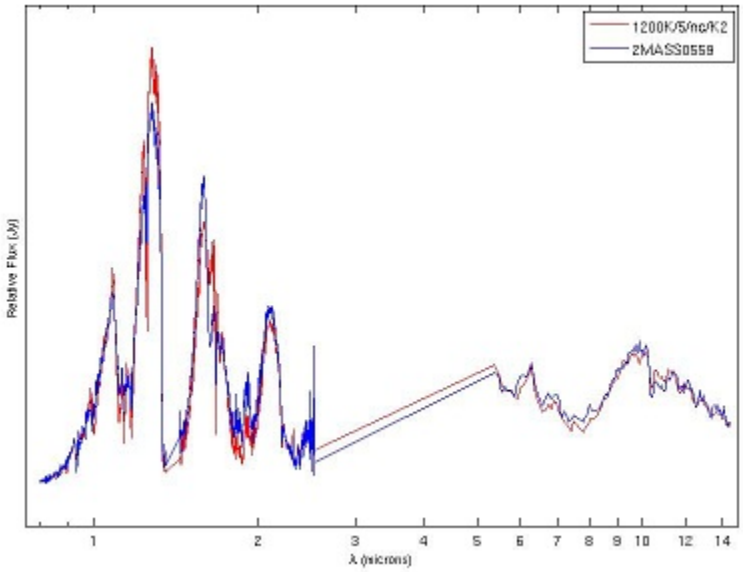

Figure 3.1 Best single fit. Model 1200K, log g 5, nc, K2.

3.2 Single Fitting

2M0559 had previously been fit by both a single and binary model [3]. The first iteration of model fitting was to attempt verification of published results. I wrote a simple minimizing routine in Matlab to solve for which out of the 1184 models best matched the observed spectra (see appendix A.5.1 and A.5.2). (In this case $\mathbf{x}$ and $\mathbf{f}_i$ were one dimensional vectors.) The best fit had parameters of 1200K, 5, nc, and K2 (T_{eff}, log g, f_{sed}, K_{zz}) (see Fig. 3.1 and 3.2). G value was 320.5957 for the over-smoothed models. This is a close match with published data (1200K, 4.5, nc, K2). Only the gravity is different and the model with 4.5 log g is in the top five single fits.

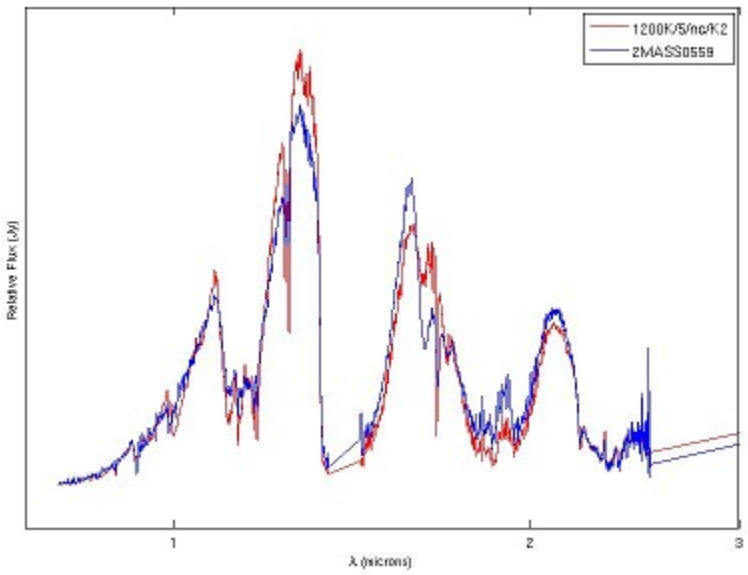

Figure 3.2 Best single fit. Detail on near-infrared range.

3.3 Double Fitting

A binary fit was attempted using two equal dwarf systems. However, due to the nature of the the minimizing routine, this returned the same best fit model and G value. In Stephens et al. 2009 [3] a best fit of an equal system was 1200K, 5.5, f4, K4 (T_{eff}, log g, f_{sed}, K_{zz}). The discrepancy is of little consequence however, as the fitting procedure done in the previous analysis used a fixed $\mathbf{x}$ value calculated from estimated radii and known distance. This present analysis was fitting spectral shape only and not distance. Thus this analysis moved the double system further away by lowering $\mathbf{x}$ and returned the same best fit.

Next, a best fit for unequal systems was attempted. The Matlab program was essentially the same as the single fit with a one dimensional $\mathbf{x}$ vector. The model ($\mathbf{F}_i$) however, was a straight addition of two model spectra. The models were constructed with the same distance parameters so weighting between the models is unnecessary. Using the over-smoothed models, a simple permutation of each model was paired with every other model and fit to the

Table 3.1 Top 10 binary fits

Model 1	Model 2	Gvalue
1000K 4.25 f2 K0	1300K 5.5 nc K0	237.05285
1000K 4.5 f2 K0	1300K 5.5 nc K0	237.32766
1000K 4 f2 K0	1300K 5.5 nc K0	237.5488
1000K 4.75 f2 K0	1300K 5.5 nc K0	237.56464
1000K 5 f2 K0	1300K 5.5 nc K0	239.89513
1200K 5.5 nc K0	1200K 4.5 f4 K0	247.66023
1100K 5 f3 K0	1200K 5.5 nc K0	249.53366
1200K 5.5 nc K2	1200K 4.5 f4 K0	250.1248
1300K 5.5 nc K0	900K 4.5 nc K6	250.89101
1100K 5 f3 K0	1200K 5.5 nc K2	251.05549

spectra. This amounts to 700366 different possible pairs. The best G value for all combinations was 122.05. Taking the square root of this number (11.068) and using it as a measure of deviation, the best 49 fits were chosen (those within on deviation of 122.05). Out of these 49 matches, only 33 out of the original 1184 single models were selected and two models appeared as the primary companion in 33 of the 49 matches. Both these models have a T_{eff} of 1300K, log g of 5.5, and a f_{sed} of nc. The K_{zz} value was K0 in one and K2 in the other (see Table 3.1 for the top 10 binary fits).

As the variable $\mathbf{x}$ is dependent on the dwarf's radius as well as distance a fine-tuned fitting needed a two dimensional $\mathbf{x}$ (see appendix A.5.3). In the original definition of the G1, $\mathbf{x}$ was multiplied to the model instead of the data flux. Consequently the w_i term was changed to the wavelength divided by the mean of the data flux. Hence a new statisitic was

used as defined by equation 3.2.

$$G2 = \sum_i w_i (f_i - \mathbf{x} \ . \ \mathbf{F_i})^2 \tag{3.2}$$

This will return the the same minimum but will evaluate to a significantly different G value.

The five top binary fits are also seperated from the other 49 models by a G2 value at least 10 lower than the rest (see Table 3.1). As the standard deviation of all 49 fits was 8.5542, these five model sets are a significant grouping. All five best fits include one model with parameters of 1300K, 5.5 g, nc, and K0. This model was one of the two models indentified in the large scale fitting and is therefore the best fit for the primary of this system. The other five models fitting the secondary are very similar. Three parameters are the same: 1000K, f2, and K0 (see Figs. 3.3, 3.4, 3.5, and 3.6). The only variance is in the gravity parameter with values ranging from 4.0 to 5.0. (For comparison of single and double fit systems see Fig. 3.7.) It is not surprising that it is difficult to constrain gravity because of gravity measurement's dependence on the band from 1.5 to 1.7μm which is poorly modeled (see chapter 4).

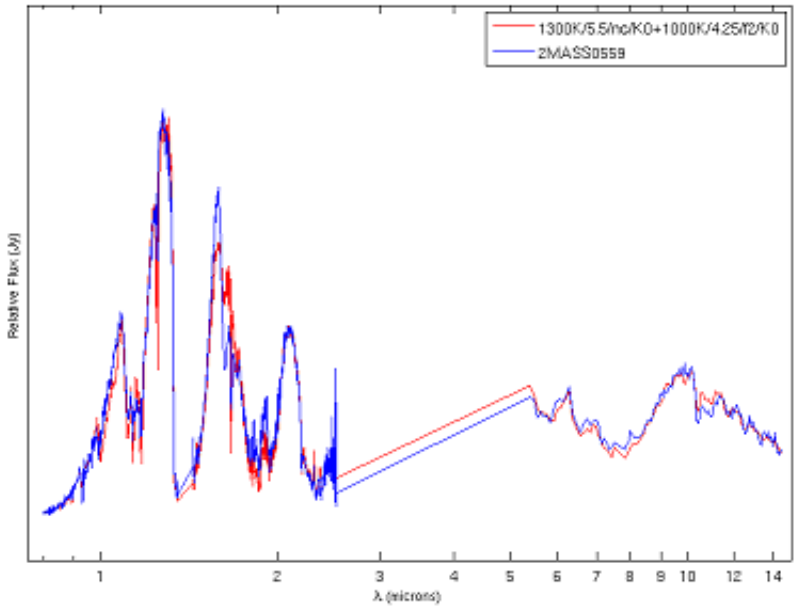

Figure 3.3 Best binary fit full spectrum. 1300K/5.5/nc/K0 + 1000K/4.25/f2/K0.

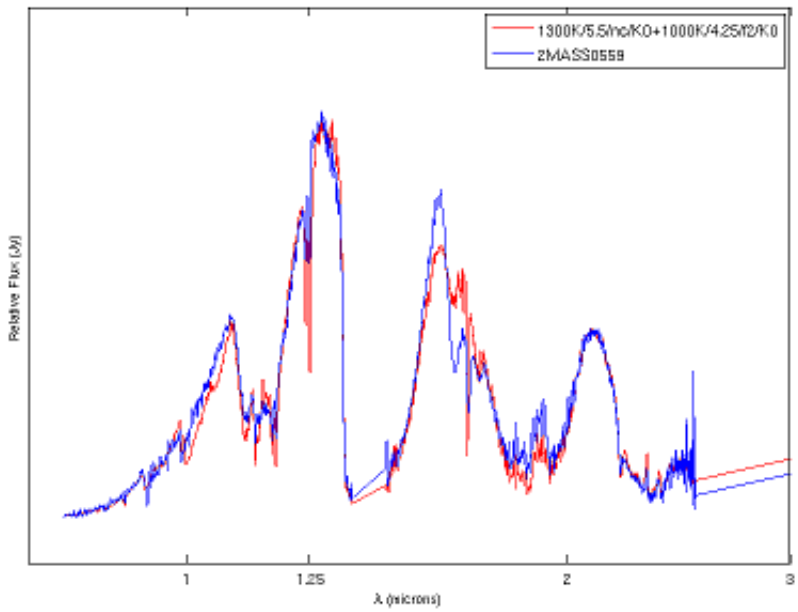

Figure 3.4 Best binary fit detail of near-infrared. 1300K/5.5/nc/K0 + 1000K/4.25/f2/K0.

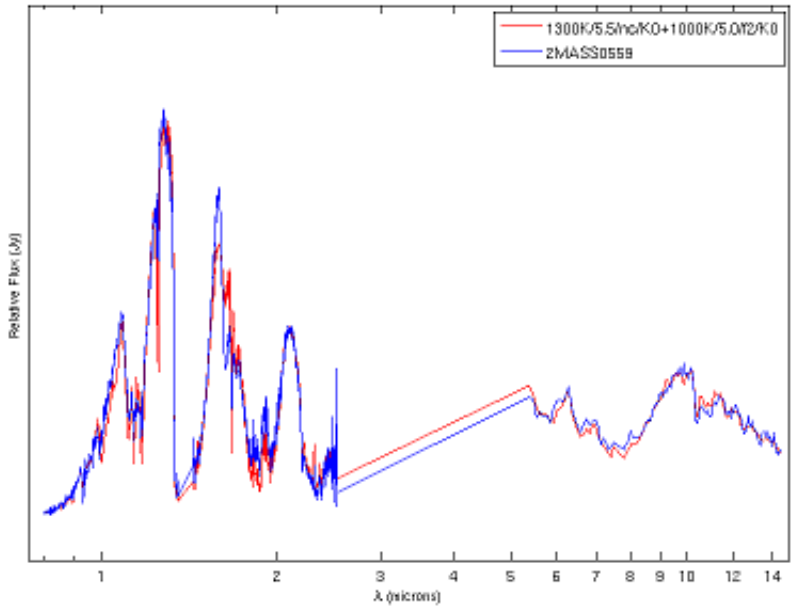

Figure 3.5 5^{th} best binary fit full spectrum. 1300K/5.5/nc/K0 + 1000K/5/f2/K0.

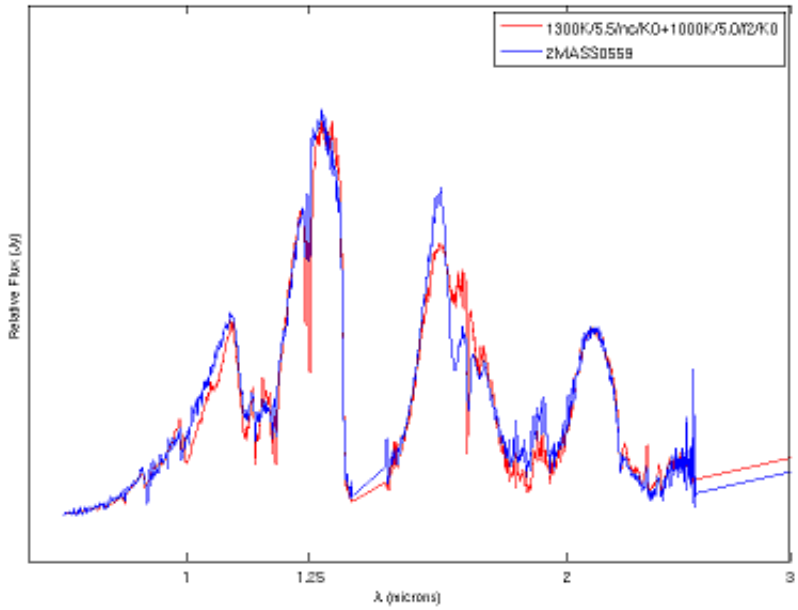

Figure 3.6 5^{th} best binary fit detail of near-infrared. 1300K/5.5/nc/K0 + 1000K/5/f2/K0.

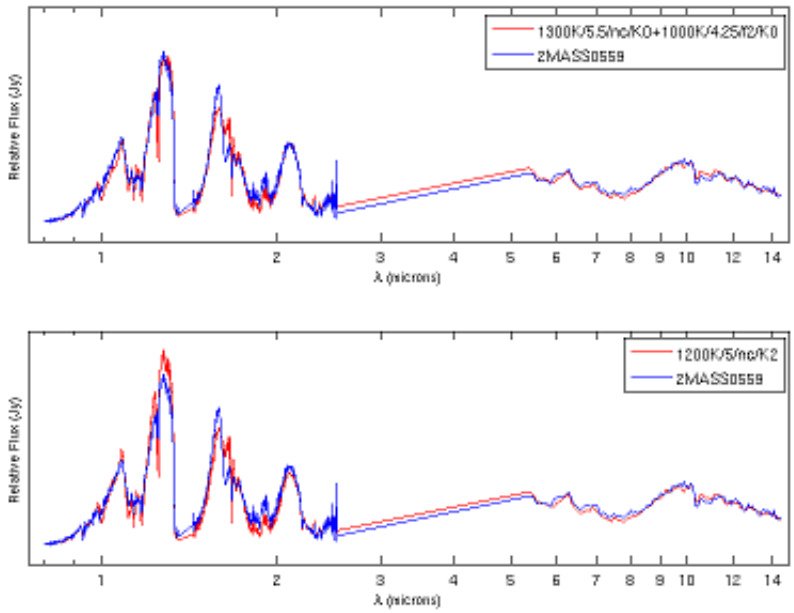

Figure 3.7 Comparison of the best single and binary fits. The best binary fit is the top graph and the bottom is the best single fit.

Chapter 4

Discussion

The system of 2M0559 has been successfully fitted to a binary system of unequal temperature models. A single fit statistically (and visually) is not adequate for explaining the observed spectra. The single fit not only served as a verification of published results but allowed a statistical basis of comparison. As the minimizing routine was identical for the first iteration of binary system and single fitting a direct comparison of G1 values is allowed. The single fit G1 value of 320.5957, when compared to the double system sits at about 16000^{th} from the lowest score of 122.0527.

It is known, however, that the models have flaws. An examination of the model spectra around 1.62μm clearly doesn't match observation. This discrepancy is due to CH_4 bands known to exits, but as yet have not been replicated in the lab and therefore cannot included in the models. Also at 1.25μm a fine absorption double line is clearly too deep to match spectra. However, both of these instances merely indicate the need for further model refinement. These mistaken features are found in all the models and therefore only give an overall bias to the statistical analysis. The returned G values, though artificially higher, are differentially compared and the bias is eliminated.

A surprising result found among the fits is the presence of a relatively high cloud f_{sed}

value in the secondary in the system. As all five top fits include this parameter it cannot be ignored. Previous studies have shown that as the transition from L to T dwarfs is made, the clouds get progressively thinner [10] [11] until the cloud condensation is no longer needed to model the spectra. This has been concluded theoretically as well, with the suggested cut off limit for loss of clouds due to depth in the photosphere at ≈1000K [12]. As the temperature gets cooler, clouds are still formed but are too low in the atmosphere to effect opacity. The secondary sits right on this limit yet has a f_{sed} parameter of f2. We looked at the other top binary fits to find the best fit within the bounds of accepted theory. However, this match was obviously not correct visually. Dr. Stephens and I both concluded that the G value found binary fit should be presented, otherwise the statistical analysis would have been pointless. Thus we are forced to conclud that the theory of cloud formation needed revision.

In the past few months, another publication has come to this same conclusion. Burgasser et al. 2010 [13] found it essential to include clouds in the spectral model fitting of a late T dwarf with a T_{eff} of 650K. Clearly this object was outside the theoretical limit for cloud opacity. Burgasser even gives a hypothesis to explain this discrepancy: the presence of clouds is due to the objects low gravity. He gives two arguments to support his hypothesis. First, the Ackerman and Marley 2001 [9] models predict a larger grain size in lower gravity systems. Though the clouds are deeper, larger particles are more effective at scattering and absorption. Second, if a measurement is taken from a fixed pressure level in the atmospheres of two dwarfs differing only in gravity, the column of atmosphere above is larger in volume for the lower gravity. As optical length is a function of density, this is essentially how a spectrum is measured. Thus pressure for pressure the lower gravity dwarf has a warmer column and clouds will form higher in the atmosphere. Burgasser noticed that the late T dwarfs that have been fit without high cloud opacity are systems with log g values of 5 or above. This correlation of low gravity to higher clouds in L dwarfs can be seen in Cushing

et al. 2008 [10] and one example of a T dwarf in Stephens et al. 2009 [3]. This last T dwarf had a log g of 4.5 but an f_{sed} value of 4. This cloud parameter is still rather small and is only an indication that such a correlation exists. Interestingly, the top five double fits include the gravity parameter of 4.0, 4.25, 4.5, 4.75, and 5.0 all very low gravity and the 5.0 model (highest gravity) is the 5^{th} best fit. Fitting these parameters would conclude that this system collaborates Burgasser's hypothesis.

By accepting the lower gravity for secondary, the entire system's gravity needs to be examined. A binary system is assumed to have both components form at the same time. Without active fusion, the dwarf will contract over time thus increasing the gravity with age. Burgasser et al. 2010 [13] notes that his hypothesis is for young and cold dwarfs. For 2M0559 to fit the proposed explanation, it needs to be shown that the system is young. I conducted further research and found that as an unequal luminosity (and hence mass) system evolves through time that gravity values increase for both members approaching the same value. However, this increase is quicker for the higher mass object (eg. [2]). Thus for a young binary system, the lower mass (less luminous, mass, and temperature) is expected to have a lower gravity. This is what is found from the present analysis.

The G values and graphs of the 1^{st} and 5^{th} best fit (Figs. 3.3, 3.4, 3.5, and 3.6) show only minor feature differences. To distinguish between these top fits, fine feature fitting is essential and unfortunately as discussed earlier the models are not accurate enough. Fitting with known distance and predicted radius also does not distinguish between these five fits. It is possible to conclude that the gravities for both the primary and secondary are somewhere between 5.0 and 5.5 as this is one discrete step for the modeling parameters. However, it would be expected then that the model of 1000K, 5.5, f2, K0 would be near this cluster of fits and it is not (it isn't even in the top 49). In addition, if we suppose that the gravities are equal there is no longer an explanation for the clouds present in the less luminous body.

We conclude that the gravities are unequal with the smaller object log g approximately 4.5.

Further research being done by the research group has resolved the primary and secondary visually in data taken from Hubble Space Telescope [14]. In connection with the present study the overluminous system 2M0559 has been shown to fit an young unequal-mass binary system. Intriguing new evidence is emerging for young late T dwarfs exhibiting cloud opacity. Further study and theoretical modeling will be needed to establish the exact parameters of this unique system.

Appendix A

MatLab Programs

A.1

Mask1.m for making masks files on a set of images.

```
clear all; close all;
%making masks and specfix files for a list of csv files for a set of images
q=input('name of file with list of csv files? ', 's');
k=input('what is # for bp#.txt? ', 's');
%get rid of the next two line and un % the s and k above
%s='bp2.txt';
%k='2';
[names]=textread(q,'%s'); %loading the list of names that you want...
N=length(names);
for n=0:N-1 %making a full matrix of the median values each column corresponds to the
%value of the pixel for each file starting at 0
    s=strcat('000',num2str(n));
```

```
    s1=s(end-2:end);
    temp=load (['bp',k,'.',s1,'.csv']);
    allmatrix(:,n+1)=temp(:,3);
end
xpixel(:,1)=temp(:,1); ypixel(:,1)=temp(:,2); %these are the x and y pixel values to be used
%later.
numpix=length(xpixel);
%now constructing a median and std array called medianall and stdall
medianall=zeros(numpix,1);
stdall=zeros(numpix,1);
for n=1:numpix
    medianall(n,1)=median(allmatrix(n,:));
    stdall(n,1)=std(allmatrix(n,:));
end
i=0;
term=0;
while term < numpix %this is a array of the pixels that we don't want to use we will also
%find the width of medians to use for the "good statistics"
    term=term+1;
    if medianall(term,1)==0
      i=i+1;
      badpix(i)=term;
    else
      medtemp(term-i,1)=medianall(term,1);
    end
```

```
end
g=median(medtemp); g1=g+5*std(medtemp); g2=g-5*std(medtemp);
term=0;
i=0;
l=0;
while term < numpix %this will give the good pix for std evaluation
    %also created is a list of good pixels named goodpix
    term=term+1;
    if l+1<=length(badpix)
      if term==badpix(l+1)
      l=l+1;
      else
          if medianall(term,1)<g1 && medianall(term,1)>g2
      i=i+1;
      goodpix(i,1)=term;
      goodpixstd(i,1)=stdall(term,1);
          end
      end
    else
      if medianall(term,1)<g1 && medianall(term,1)>g2
          i=i+1;
          goodpix(i,1)=term;
          goodpixstd(i,1)=stdall(term,1);
      end
    end
```

```
end
sttotal=5*std(goodpixstd); %this is the 5 sigma value for the data set using only the good
%pixels
n=1; m=1;
ifthen=zeros(numpix,N);
for m=1:N %this constructs the if then matrix to see if the pixel is off of the median value
    for n=1:numpix
      if abs(medianall(n,1)-allmatrix(n,m))>sttotal
          ifthen(n,m)=1;
      end
    end
    n=1;
end
sumc=zeros(numpix,1);
for n=1:numpix % sumc is a list of the number of times the if then returned a bad value
    sumc(n)=sum(ifthen(n,:));
end
term=0;
i=0;
while term < numpix
    term=term+1;
    if sumc(term)> 0.25*N
      i=i+1;
      mask(i,1)=xpixel(term); mask(i,2)=ypixel(term);
    end
```

```
end
fid = fopen(['mask',k,'.txt'], 'w'); %this creates the all bad pixels (greater than 75% of
%number of frames) called mask*.txt where * is the value k
fprintf(fid, '%0.0f %6.0f\n', mask.');
fclose(fid);
m=1;
for m=1:N
term=0;
i=0;
o=1;
masktemp=0;
specfixtemp=0;
    while term < numpix %now we make the individual mask files
    term=goodpix(o);
      if ifthen(term,m)==1
          i=i+1;
          masktemp(i,1)=xpixel(term,1);
          masktemp(i,2)=ypixel(term,1);
          specfixtemp(i,2)=ypixel(term,1);
          specfixtemp(i,1)=xpixel(term,1);
          specfixtemp(i,3)=medianall(term);
      end
      o=o+1;
    end
s=strcat('000',num2str(m-1));
```

```
s1=s(end-2:end);
fid = fopen(['mask',k,'.',s1,'.txt'], 'w'); %this creates the individual mask files
fprintf(fid, '%0.0f\t %0.0f\n', masktemp.');
fclose(fid);
fid = fopen(['specfix',k,'_',s1,'.txt'], 'w'); %this creates the individual specfix files
fprintf(fid, '%0.0f\t %3.0f\t %0.7f\n', specfixtemp.');
fclose(fid);
end
```

A.2

smoothing.m (taking a variable boxcar average)

```
forb=1:1184
   b1=num2str(b);
model=load (['model', b1, '.txt']);
clear temp;
for m=1:length(model)
templam=model(m,1);
dlam=templam/120;
up=templam+1/2*dlam;
down=templam-1/2*dlam;
temp(m,1)=model(m,1);
i=0; clear tbin
   forn=1:length(model)
      if down <= model(n,1) && up >= model(n,1)
```

```
        i=i+1;tbin(i,1)=model(n,2);
      end
   end
temp(m,2)=sum(tbin)./length(tbin);
end
fid = fopen(['tmodel', b1,'.txt'],'w');
fprintf(fid, '%0.8f\t %0.6g\n', temp.');
fclose(fid);
end
```

A.3

smoothingdouble.m (taking a variable boxcar average)

```
clear all;
for b=1:1184
    b1=num2str(b);
% model2=load (['model', b1, '.txt']);
model=load (['model', b1, '.txt']);
%model=load('model1.txt');
clear temp;
for m=1:length(model)
templam=model(m,1);
dlam=templam/400; %this is one resolution
up=templam+1/2*dlam;
down=templam-1/2*dlam;
```

```
dlam2=templam/60; %this is another resolution
up2=templam+1/2*dlam2;
down2=templam-1/2*dlam2;
temp(m,1)=model(m,1);
i=0; clear tbin
    for n=1:length(model)
        if model(n,1) < 3
        if down <= model(n,1) && up >= model(n,1)
          i=i+1;tbin(i,1)=model(n,2);
        end
        else
          if down2 <= model(n,1) && up2 >= model(n,1)
            i=i+1;tbin(i,1)=model(n,2);
          end
        end
        end
    temp(m,2)=mean(tbin);
    end
    fid = fopen(['a1model', b1,'.txt'],'w');
    fprintf(fid, '%0.8f\t %0.6g\n', temp.');
    fclose(fid);
    end
```

A.4

binning2.m for binning models to compare to data spectra

```
clear all; close all;
temp=load ('allFlamdatawithoutfitting.txt');
for b=1:1184
    r=1;
    b1=num2str(b);
    model2=load (['tmodel', b1, '.txt']);
clear newmodel2
for m=287:1139
k=temp(m,1);
k1=abs((temp(m-1,1)-temp(m,1))/2);
k2=abs((temp(m,1)-temp(m+1,1))/2);
up=k+abs((temp(m,1)-temp(m+1,1))/2);
down=k-abs((temp(m-1,1)-temp(m,1))/2);
%I make bins that center around the point in the data
i=0;
clear tbin
    for n=1:length(model2)
        if down <= model2(n,1)&& up >= model2(n,1)
          i=i+1;tbin(i,1)=model2(n,2);tbin(i,2)=model2(n,1);
        end
    end
newmodel2(r,1)=k;
newmodel2(r,2)=sum(tbin(:,1))./length(tbin);
```

```
r=r+1;
end
%This section is just to find the end point before the jump I will repeat
%this for each end... do not be alarmed
m=1140;
k=temp(m,1);
k1=abs((temp(m-1,1)-temp(m,1))/2);
up=k+k1;
down=k-k1;
i=0;
clear tbin
    for n=1:length(model2)
        if down <= model2(n,1)&& up >= model2(n,1)
          i=i+1;tbin(i,1)=model2(n,2);tbin(i,2)=model2(n,1);
        end
    end
newmodel2(r,1)=k;
newmodel2(r,2)=sum(tbin(:,1))./length(tbin);
r=r+1;
m=1141;
k=temp(m,1);
k1=abs((temp(m+1,1)-temp(m,1))/2);
up=k+k1;
down=k-k1;
i=0;
```

```
clear tbin
    for n=1:length(model2)
        if down <= model2(n,1)&& up >= model2(n,1)
          i=i+1;tbin(i,1)=model2(n,2);tbin(i,2)=model2(n,1);
        end
    end
newmodel2(r,1)=k;
newmodel2(r,2)=sum(tbin(:,1))./length(tbin);
r=r+1;
for m=1142:2453
k=temp(m,1);
k1=abs((temp(m-1,1)-temp(m,1))/2);
k2=abs((temp(m,1)-temp(m+1,1))/2);
up=k+abs((temp(m,1)-temp(m+1,1))/2);
down=k-abs((temp(m-1,1)-temp(m,1))/2);
i=0;
clear tbin
    for n=1:length(model2)
        if down <= model2(n,1)&& up >= model2(n,1)
          i=i+1;tbin(i,1)=model2(n,2);tbin(i,2)=model2(n,1);
        end
    end
newmodel2(r,1)=k;
newmodel2(r,2)=sum(tbin(:,1))./length(tbin);
r=r+1;
```

```
end
m=2454;
k=temp(m,1);
k1=abs((temp(m-1,1)-temp(m,1))/2);
up=k+k1;
down=k-k1;
i=0;
clear tbin
    for n=1:length(model2)
        if down <= model2(n,1)&& up >= model2(n,1)
          i=i+1;tbin(i,1)=model2(n,2);tbin(i,2)=model2(n,1);
        end
    end
newmodel2(r,1)=k;
newmodel2(r,2)=sum(tbin(:,1))./length(tbin);
r=r+1;
m=2455;
k=temp(m,1);
k1=abs((temp(m+1,1)-temp(m,1))/2);
up=k+k1;
down=k-k1;
i=0;
clear tbin
    for n=1:length(model2)
        if down <= model2(n,1)&& up >= model2(n,1)
```

```
            i=i+1;tbin(i,1)=model2(n,2);tbin(i,2)=model2(n,1);
        end
    end
newmodel2(r,1)=k;
newmodel2(r,2)=sum(tbin(:,1))./length(tbin);
r=r+1;
for m=2456:2582
k=temp(m,1);
k1=abs((temp(m-1,1)-temp(m,1))/2);
k2=abs((temp(m,1)-temp(m+1,1))/2);
up=k+abs((temp(m,1)-temp(m+1,1))/2);
down=k-abs((temp(m-1,1)-temp(m,1))/2);
i=0;
clear tbin
    for n=1:length(model2)
        if down <= model2(n,1)&& up >= model2(n,1)
            i=i+1;tbin(i,1)=model2(n,2);tbin(i,2)=model2(n,1);
        end
    end
newmodel2(r,1)=k;
newmodel2(r,2)=sum(tbin(:,1))./length(tbin);
r=r+1;
end
m=2583;
k=temp(m,1);
```

```
k1=abs((temp(m-1,1)-temp(m,1))/2);
up=k+k1;
down=k-k1;
i=0;
clear tbin
    for n=1:length(model2)
        if down <= model2(n,1)&& up >= model2(n,1)
          i=i+1;tbin(i,1)=model2(n,2);tbin(i,2)=model2(n,1);
        end
    end
newmodel2(r,1)=k;
newmodel2(r,2)=sum(tbin(:,1))./length(tbin);
fid = fopen(['bmodel', b1,'.txt'],'w');
fprintf(fid, '%0.8f\t %0.6g\n', newmodel2.');
fclose(fid);
end
```

A.5

A.5.1

m file for single fitting routine

```
global data m
data=load('data.txt');
a=1;
b=0;
```

```
lsval=zeros(1184,2);
for n=1:1184
    n1=num2str(n);
    m1=load ['bmodel', n1, '.txt']);
    m(:,1)=data(:,1);
    m(:,2)=a*m1(:,2);
    d(:,1)=data(:,1);
    d(:,2)=data(:,2)*10^22.5;
    x=fminsearch(@lsq, 22.1);
    lsval(n,1)=n; lsval(n,2)=lsq(x);
end
[Y, I]=min(lsval);
I(1,2)
```

A.5.2

m file of function lsq used in A.5.1

```
function f = lsq(x)
global m data
f = sum((data(:,1).*1./(mean(m(:,2))).*(m(:,2)-10^22*x(1).*data(:,2))).^2);
```

A.5.3

m file of function lsq1 used in double fitting

```
function f = lsq1(x)

global m1 data m2

f = sum((data(:,1)./(mean(data(:,2))).*(-x(1)^2./(1.01E29)*m1(:,2)-x(2)^2./(1.01E29)*m2(:,2)+data(:,2))).^2);
```

Bibliography

[1] T. J. Dupuy, M. C. Liu, and M. J. Ireland, "Testing substellar models with dynamical mass measurements," EPJ Web of Conferences, (2009).

[2] M. C. Liu, T. J. Dupuy, and S. K. Leggett, "Discovery of a highly unegual-mass binary T dwarf with Keck laser guide star adaptive optics: a coevality test of substellar theoretical models and effective temperatures," ApJ. **722,** 311–328 (2010).

[3] D. C. Stephens et al., "The 0.8-14.5 μm spectra of mid-L to mid-T dwarfs: diagnostics of effective temperature, grain sedimentation, gas transport, and surface gravity," ApJ. **702,** 154–170 (2009).

[4] A. J. Burgasser et al., "Discovery of a bright field methane (T-type) brown dwarf by 2MASS," AJ. **120,** 1100–1105 (2000).

[5] C. C. Dahn et al., "Astrometry and photometry for cool dwarfs and brown dwarfs," ApJ. **124,** 1170-1189 (2002).

[6] A. D. Burgasser, J. D. Kirkpatrick, J. Liebert, and A. Burrows, "The spectra of T dwarfs. II. red optical data," ApJ. **594,** 510–524 (2003).

[7] "Spitzer Telescope Handbook," http://ssc.spitzer.caltech.edu/spitzermission/missionoverview/spitzertelescopehandbook/18/#_Toc255466023 (Accessed December 4, 2010).

[8] D. Saumon and M. M. Marley, "The evolution of L and T dwarfs in color-magnitude diagrams," ApJ. **689,** 1327–1344 (2008).

[9] A. S. Ackerman and M. S. Marley, "Precipitating condensation clouds in substellar atmospheres," ApJ. **556,** 872–884 (2001).

[10] M. C. Cushing et al., "Atmospheric Parameters of field L and T dwarfs," ApJ. **678,** 1372–1395 (2008).

[11] M. S. Marley et al., "Clouds and chemistry: ultracool dwarf atmospheric properties from optical and infrared colors ApJ. **568,** 335–342 (2002).

[12] A. Burrows, D. Sudarsky, and I. Hubeny, "Theory for the secondary eclipse fluxes, spectra, atmospheres, and light curves of transiting extrasolar giant planets," ApJ. **650,** 1140–1149 (2006).

[13] A. J. Burgasser et al., "Clouds in the coldest brown dwarfs: fire spectroscopy of ROSS 458C," Accepted in ApJ. 28, Sep. 2010.

[14] "Unpublished research done in Stephens Group."